Available online at www.sciencedirect.com

ScienceDirect

Procedia Engineering 97 (2014) 767 – 774

Procedia Engineering

www.elsevier.com/locate/procedia

12th GLOBAL CONGRESS ON MANUFACTURING AND MANAGEMENT, GCMM 2014

Optimization of the Pulsed Current Gas Tungsten Arc Welding Process Parameters for alloy C-276 using the Taguchi Method

Manikandan M,[a]* Nageswara Rao M [a], Ramanujam R [a], Devendranath Ramkumar [a], Arivazhagan N [a], Reddy G.M[b]

School of Mechanical and Building Sciences, VIT University,Tamil Nadu, 632 014, India
[b]DMRL, Hyderabad,500 058, India

Abstract

In the present work, a Design Of Experiment (DOE) technique, the Taguchi method was employed to bead on welding trials to optimize Pulsed Current Gas Tungsten Arc (PCGTA) welding process parameters of alloy C-276. A L_9 orthogonal array of Taguchi design involving nine experiments for four parameters (pulsed current, background current, % on time, pulse frequency) with three levels was used. An analysis of the mean of signal-to-noise (S/N) ratio indicates that the depth of current is influenced significantly by the levels in the Taguchi orthogonal array. The higher the better response category was selected to obtain optimum conditions for depth of penetration. The optimum conditions were found to be 165 A pulse current, 77 A background current, 60 % on time and 5 Hz pulse frequency. Analysis of Variance (ANOVA) is performed to measure percentage contribution of each factor. The results show that the pulse current was most influencing parameter on the depth of penetration and % on time (23.28 %) the next most influencing. Confirmation test was carried out to validate the results of Taguchi analysis; the result shows that there is good match between expected and predicted results.

Selection and peer-review under responsibility of the Organizing Committee of GCMM 2014

Keywords: Alloy C-276, Taguchi method; Design of experiments; Analysis of variance; Pulsed current gas tungsten arc welding

* Corresponding author. Tel.: +91 9944681416; fax: +91-416-2243092.
*E-mail address:*mano.manikandan@gmail.com

Selection and peer-review under responsibility of the Organizing Committee of GCMM 2014
doi:10.1016/j.proeng.2014.12.307

1. Introduction

Nickel based superalloy C-276 is distinguished by its high corrosion resistance to a large spectrum of aggressive environments encountered in industry [1]. The nickel matrix of the alloy enables to accommodate high percentages of elements such as chromium, iron, molybdenum etc., while retaining single phase face-centred-cubic structure [2]. The welding of alloy C-276 is beset with some problems. Cieslak et al. [3] carried out arc welding studies on alloys C-4, C-22, and C-276. All these grades are highly corrosion resistant nickel- base alloys derived from Ni-Cr-Mo ternary system. The authors found that elemental segregation occurs during welding, leading to the formation of brittle Topologically Close Packed (TCP) phases P and μ in alloys C-22 and C-276 [3]. In addition, the authors reported that alloy C-276 shows the highest susceptibility to hot cracking among the three alloys. Precipitation of intermetallic phase P, μ and carbides has been observed in commercial grade alloy C-276 [1, 4 and 5]. The major issue in the welding of alloy C-276 is to reduce the susceptibility of hot cracking during welding. This can be achieved by avoiding the formation of these intermetallic phases. This in turn can be realized if one can cut down on the severity of microsegregation occurring during fusion welding. In this context pulsed current GTA mode has shown some promise. For example Guangyi et al. [6] reported that microsegregation in alloy C-276 joints produced by pulsed laser beam welding is relatively less compared to the situation obtained with arc welding process. Manikandan et al.[7] compared the quality of weldments produced by constant current Gas Tungsten Arc Welding (CCGTAW)henceforth referred as GTAW and Pulsed Current Gas Tungsten Arc Welding (PCGTAW) in superalloy 718 and concluded that the latter mode achieved maximum instantaneous cooling rate leading to reduction in the amount of deleterious Laves phase in the fusion zone. Manikandan et al. [8] compared the quality of weldments produced by GTAW and PCGTAW in alloy C-276 and the results show that pulsing results in refined microstructure, reduced microsegregation and improved strength of weld joint. Manikandan et al. [9] adopted the continuous Nd: YAG laser welding of alloy C-276 and showed that the reduced segregation in the fusion zone and improved mechanical property. Pulsed current gas tungsten arc welding (PCGTAW) is a variation of GTAW. PCGTAW involves cycling of the welding current from a high level (pulse current) to a low level (background current) at a selected frequency. The pulse current is generally selected to give adequate penetration and bead contour, while the background current is set at a level sufficient to maintain a stable arc. Unlike in GTAW, during PCGTAW the heat energy required to melt the base material is supplied only during peak current pulses for brief intervals of time; this allows the heat to dissipate into the base material leading to a narrower Heat Affected Zone (HAZ). The PCGTAW has many other advantages over GTAW, such as enhanced arc stability, increased weld depth to width ratio, refined grain size, reduced porosity, low distortion and better control of heat input [10].

It can be seen from the published literature that weld structure of alloy C-276 have a wider range of applications in naval and other industries. It is also observed that very limited work has been reported on welding of alloy C-276. There is no published literature on the influence of process parameters on depth of penetration and weld bead geometry of alloy C-276 when autogenous PCGTAW technique is adopted.

The purpose of the present research is to identify the optimum combination of process parameters for PCGTA welding to obtain high depth of penetration with fine bead geometry.

2. Experimental Procedure

The material chosen for the present study was a 4 mm thick plate of alloy C-276; it was received in hot rolled condition. The chemical composition is given in Table 1.

Table 1 Chemical composition of base metal (% Wt.)

Mo	Cr	W	Co	Mn	Fe	Ni	Others
16.36	15.83	3.45	0.05	0.41	6.06	Bal	0.17 (V), 0.005(P), 0.002 (S), 0.02 (Si), 0.005(C)

The welding trials were carried out manually using KEMPI DWE welding machine, and PCGTAW process. The welding parameters were designed by using Minitab-16. The Taguchi designs for welding parameters are shown in Table 2. Henceforth the parameters pulse current, background current, % on time and pulse frequency are referred to as A, B, C and D respectively. The plates are cleaned with acetone before subjected to welding. High purity argon was used as a shielding gas with a flow rate of 15 l/min. Cross sectional macrostructure examination was carried out to look for any macro deficiencies and to determine the depth of penetration.

Fig. 1 Bead on Plate welding Tracks

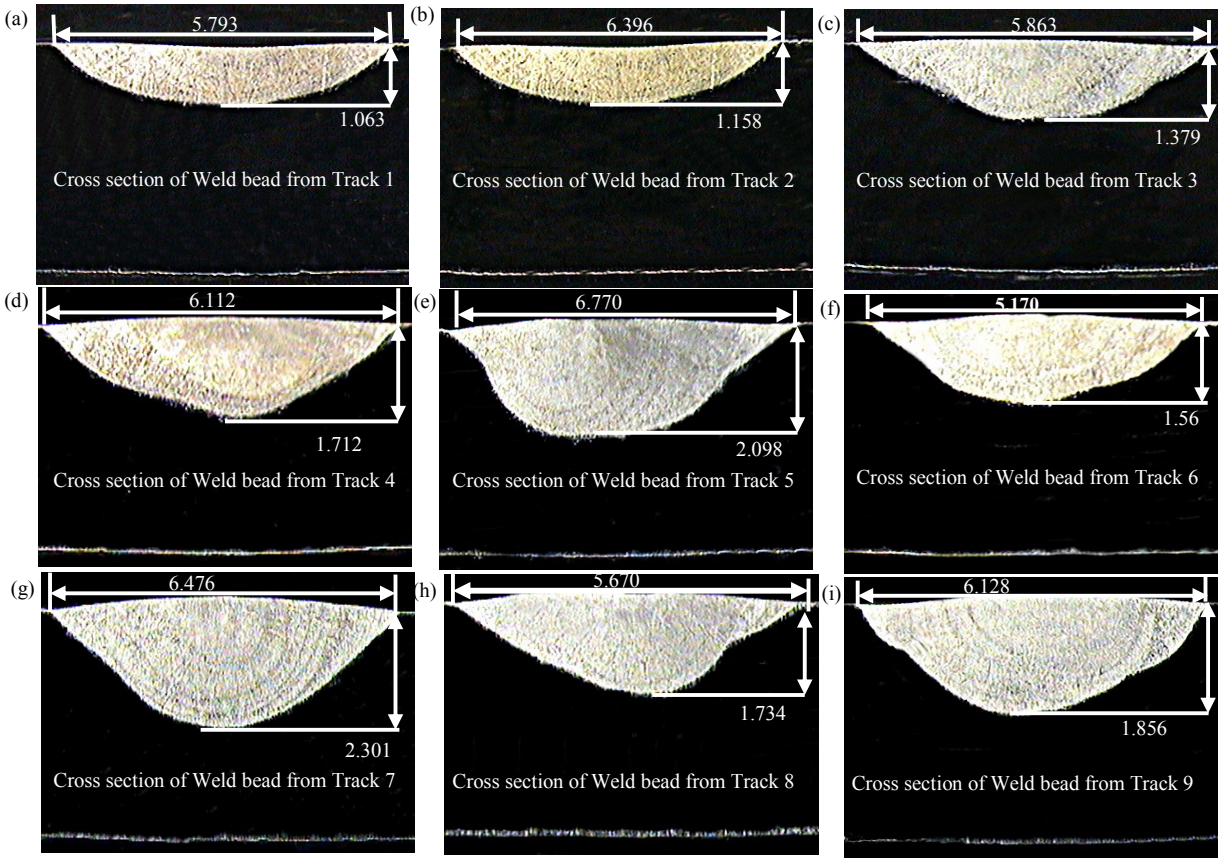

Fig. 2 Macrographs of weld beads

Table 2 Design factor and levels

Parameters	Code	Levels		
		1	2	3
Pulse current, A	A	145	155	165
Background current, A	B	72	77	82
% on time	C	40	50	60
Pulse frequency, Hz	D	4	5	6

3. Taguchi Design of Experiment

The Taguchi method uses special orthogonal arrays to study all the design factors with minimum of experiments [11]. Orthogonality means that each factor is independently evaluated and the effect of one factor does not interfere with estimation of the influence of another factor [11, 12]. Four factors (pulse current, background current, % on time, pulse frequency) with three levels were selected as shown in Table 2. In this present study, each factor has three levels. The DOF obtained for each factor is therefore 2. For all four factors put together the total DOF works out to 8. An L_9 (3^4) orthogonal array of Taguchi design involving nine experiments for four parameters with three levels and eight DOF was adopted for the present study.

4. Results and Discussion

4.1 Determination of optimal levels

Welding was carried out as per the design. The Fig. 1 shows the nine weld tracks produced. Macro examination of the transverse sections revealed no weld deficiency. Figure 2 shows the transverse macro sections. Depth of penetration was measured from the macro section and the results are shown in table 3.
There are three categories of quality characteristics, i.e., the higher the better (HB), the lower the better (LB) and the nominal the better (NB) [13]. In this study, depth of penetration is treated as a characteristic value. Since the depth of penetration is intended to be maximized, the S/N ratio for HB characteristics was selected, which can be calculated from the following equation (1).

$$\frac{S}{N} = -10log_{10}\left(\frac{1}{n}\sum_{i=1}^{n}\frac{1}{Y_i^2}\right) \qquad (1)$$

Where S/N is performance statistics, n is the number of repetitions for an experimental combination; and Y_i is performance value of the i^{th} experiment. In the present study for any given experimental combination only one trial was carried out hence n=1 and the equation can be rewritten as.

$$\frac{S}{N} = -10log_{10}\left(\frac{1}{Y_i^2}\right) \qquad (2)$$

The S/N ratio corresponding to L_9 orthogonal array are also included in Table 3. Then the mean S/N ratios at each level for various factors have been calculated. The optimum levels were selected as the largest S/N ratio among all the levels of the factors. In order to evaluate the influence of each factor on the depth of penetration, the S/N ratio for each factor should be computed. The S/N ratio for single factor can be calculated by averaging the values of S/N ratios at different levels [13]. For example, the mean S/N ratio for % on time at level 1 can be calculated by averaging the S/N ratios for the experiments 1, 6 and 8. The mean S/N ratio for every factor at each level is calculated similarly. The determined factor responses are listed in Table 4. Fig. 3 shows the average S/N ratio for each parameter at three levels. The results shows that the pulse current (Fig. 3a) and % on time (Fig. 3c) exhibit large variations in the present study, whereas the variations are found to be very small in background current (Fig. 3b) and pulse frequency (Fig. 3d). As seen in Fig. 3a pulse current is the most effective factor in this present study. The S/N ratio of pulse current steeply increases between 145 to155 A; the increase is not so high in the range 155 to 165 A. This is believed to be due to the well documented strong effect of the pulse current on depth of penetration.

Background current and pulse frequency are not major influencing factors, as the corresponding S/N plots (Figs. 3b and 3d) are nearly horizontal. As brought out in the Introduction Section, the pulse current plays a major role in ensuring adequacy of penetration, whereas the background current plays an essentially passive role of providing a stable arc.

Trial No	Pulse Current A	Background Current A	% on time	Pulse frequency Hz	Depth of Penetration mm	S/N ratio dB
1	145	72	40	4	1.063	0.530
2	145	77	50	5	1.158	1.274
3	145	82	60	6	1.379	2.791
4	155	72	50	6	1.712	4.670
5	155	77	60	4	2.098	6.436
6	155	82	40	5	1.560	3.862
7	165	72	60	5	2.301	7.238
8	165	77	40	6	1.734	4.780
9	165	82	50	4	1.856	5.371

Table 3 Experimental results for depth of penetration and corresponding S/N ratios

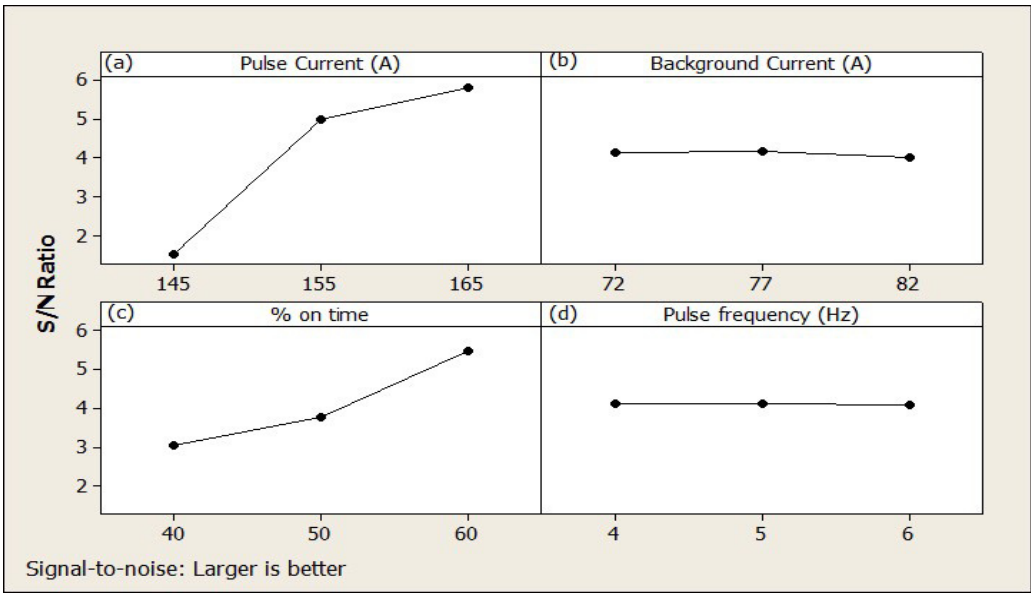

Fig. 3 The S/N response graphs for depth of penetration (a) Pulse current, (b) Background current, (c) % on time, and (d) Pulse frequency

As observed in Fig. 3(a), pulse current is the most effective factor chosen in this study on the depth of penetration. The % on time is the second most effective factor. It is seen from Fig. 3c, that S/N ratio increases with increase in % on time from 40 to 50 and the increase is even higher from 50 to 60. The maximum penetration was obtained at 60 % on time - Track 7 (Fig. 2g). It is also observed that the least depth of penetration was obtained in the case of Track 1 (Fig 2a); this is believed to be due to the low pulse current as well as low % on time. The optimum level/factor combination of PCGTA parameters is obtained by employing Taguchi method. In Table 4 the combinations A3, B2, C3 and D2 yield the highest values of S/N ratios for the factors A, B, C and D respectively. Hence, A3, B2, C3 and D2 are the optimal values of parameters for PCGTA welding. The optimal values - the peak current 165A, Background current 77A, % on time 60 and pulse frequency 5 Hz - are compiled in Table 5.

Table 4 The response table for S/N ratio

Level	Factors			
	Pulse Current (A)	Background Current (B)	% on time (C)	Pulse frequency (D)
Level 1	1.532	4.146	3.058	4.113
Level 2	4.990	**4.164**	3.772	**4.125**
Level 3	**5.797**	4.008	**5.489**	4.081
Δ (max-min)	4.265	0.155	2.431	0.044
Rank	**1**	**3**	**2**	**4**

The optimum levels of the factors are given in bold (the highest value in the column)

Table 5 Optimum process parameters

Serial no	Factors	Level	Values
1	Pulse Current (A)	3	165
2	Background Current (A)	2	77
3	% on time	3	60
4	Pulse frequency (Hz)	2	5

4.2 Analysis of Variance (ANOVA) results.

ANOVA was used to determine the influence and relative importance of the different factors. The sum of square (SS), the degrees of freedom (D), the variance (V) and the percentage of contribution to the total variation (P) are used in ANOVA, which can be calculated from the following equations (Eqs. 3-6) [13].

$$SS_T = \sum_i^m \eta_i^2 - \frac{1}{m}\left[\sum_{i=1}^m \eta_i\right]^2 \qquad (3)$$

where SS_T is the total sum of squares, m is the total number of experiments, and η_i is the S/N ratio at the i^{th} test.

$$SS_P = \sum_{j=1}^t \frac{(S_{\eta j})^2}{t} - \frac{1}{m}\left(\sum_{i=1}^m \eta_i\right)^2 \qquad (4)$$

where SS_p represents the sum of squares from the test factors, p represents one of the test factors, j the level number of this specific factor p, t the repetition of each level of factor p, and Sηj the sum of the S/N ratio involving this factor and level j.

$$V_P\,(\%) = \frac{SS_P}{D_P} \times 100 \qquad (5)$$

where V_P is the variance from the test factors, and D_P is the degree of freedom for each factor

$$P_P(\%) = \frac{SS_P}{SS_T} \times 100 \qquad (6)$$

where P_p is the percentage of the contribution to the total variation of each individual factor. The percentage contributions of each factor obtained by the ANOVA results are illustrated in Table 6.

Table 6 Results of the ANOVA for depth of penetration

Symbol	Factors	Degrees of Freedom (D)	Sum of squares (SS)	Variance (V)	Contribution (P %)	Rank
A	Pulse current	2	30.80	15.4	76.61	1
B	Background Current	2	0.04	0.02	0.10	3
C	% on time	2	9.36	4.68	23.28	2
D	Pulse frequency	2	0.00	0.00	0.00	4
Total		8	40.02		100	

ANOVA analysis showed that pulse frequency was less effective than other parameters. Pulse current and % on time are found to be more effective. Pulse current has the maximum influence on the depth of penetration with 76.61% contribution and the pulse frequency and background current was an insignificant factor with only 0.00% and 0.10 % contributions. In the ANOVA analysis, if the percentage error (P_e) contribution to the total variance is lower than 15%, no important factor is missing in the experiment design [13,14].

4.3 Confirmation test

In order to validate the methodology, a confirmation test was performed by setting the optimum conditions for four factors 165A, for peak current, 77A for background current, 60 for % on time and 5 Hz for the pulse frequency.
The predicted S/N ratio [S/N] predicted can be calculated using this combination of parameters with the following equation.

$$[S/N]_{predicted} = [S/N]_m + \sum_{i=1}^{y} ([S/N]_i - [S/N]_m) \qquad (7)$$

Where $[S/N]_m$ is the total mean S/N ratio, $[S/N]_i$ is the mean S/N ratio at the optimal level, and y is the number of main design parameters that affect the quality characteristic.
The value of $[S/N]_m$ calculated from Table 3 is 4.105. Also, $[S/N]_i$ for A3, B2, C3, and D2 can obtained from Table 4. The corresponding values are 5.797, 4.164, 5.489 and 4.125 respectively. By using these values, Eq. (7) can be solved as $[S/N]_{predicted}$=4.105+[(5.797-4.105)+(4.164-4.105)+(5.489-4.105)+(4.125-4.105)]. The $[S/N]_{predicted}$ works out to 7.26. The corresponding estimated depth of penetration was calculated using Eq. (2); it works out to 2.30. Table 7 shows good agreement between the predicted and the experimental depth of penetration.
The optimum combination of process parameters is almost matching with the parameters used for producing track 7 in the present study, except for the background current. The contribution of background current in the present study is 0 %. Figure 3b has already brought out that the background current exerts very little influence on the depth of penetration.

Table 7 Confirmation testing to validate the approach

	Parameters				S/N ratio		Performance values for Depth of Penetration (mm)	
	A Pulse Current, A	B Background Current, A	C % on time	D Pulse frequency, Hz	Prediction	Experiment	Prediction	Experiment
Optimum level	3	2	3	2	7.26	7.23	2.3	2.3
Optimum Value	165	77	60	5				

Conclusions

The major conclusions drawn from the present study are listed below

- The pulse current has the most significant influence on the depth of penetration and % on time is second most significant factor. The effects of background current and pulse frequency are very small in comparison.
- The percentage contribution of the pulse current and % on time are 76.61 %, 23.28 % respectively.
- The confirmation test demonstrated good agreement between the predicted and the experimental depth of penetration.
- The optimized welding parameters are obtained at a pulse current of 165 A, background current of 77 A, % on time of 60 and pulse frequency of 5 Hz.

Acknowledgment

This research work was supported by the Defence Research Development organization (DRDO) (Grant No ERIP/ER/1103952/M/01/1403). We also thank to Aeronautics Research and Development Board for the funding received (Grand No DARO/08/2031674/M/I) for procured KEMPI DWE welding machine used in the present study

Reference

[1] J.I. Akhter, M.A. Shaikh, M. Ahmad, M. Iqbal, K.A. Shoaib, W. Ahmad, Effect of aging on the hardness and impact properties of Hastelloy C-276. Mater. Sci. Lett. 20(2001)333-335.

[2] W.Betteridge, Nickel and its alloys, Ellis Harwood, Chichester, 1984.

[3] M.J. Cieslak, T.J. Headley, A.D. Romig, The welding metallurgy of Hastelloy alloys C4, C22, C276. Jr. Met. Trans A. 17A(1986)2035-2047.

[4] M.Raghavan, B.J. Berkowitz, J.C. Scanlon, Electron Microscopic Analysis of Heterogeneous Precipitates in Hastelloy C-276. Metall. Trans.13A(1982)979–984.

[5] H.M. Tawancy, Long-term ageing characteristics of some commercial nickel-chromium-molybdenum alloys. J. Mater. Sci.16(1981)2883–2889.

[6] M.A. Guangyi, W.U. Dongjiang, G.U.O. Dongming, Segregation Characteristics of Pulsed Laser Butt Welding of Hastelloy C-276. Mater. Trans. A. A42(2011)3853–7.

[7] S.G.K. Manikandan, D. Sivakumar, K. Prasad Rao, M. Kamaraj, Effect of weld cooling rate on laves phase formation in Inconel 718 fusion zone. J. Mater. Process. Technol. 214(2014) 358-364.

[8] M. Manikandan, N. Arivazhagan, M. Nageswara Rao, G.M. Reddy, Microstructural and Mechanical properties of alloy C-276 weldments fabricated by continuous and pulsed current gas tungsten arc welding technique. J.Manuf.Processes (2014), http://dx.doi.org/10.1016/j.jmapro.2014.08.002

[9] M.Manikandan, P.R. Hari, G.Vishnu, M. Arivarasu, K. Devendranath Ramkumar, N. Arivazhagan, M. Nageswara Rao, G.M Reddy. Investigation of Microstructure and Mechanical Properties of Super Alloy C-276 by Continuous Nd: YAG laser Welding. Procedia Materials Science 5c(2014) 2233-2241.

[10] A.A. Gokhale, D.J. Tzavaras, H.D. Brody, G.M. Ecer, Proceedings of conference on grain refinement in casting and welds, St. Louis (MO), TMS-AIME(1982)223–247.

[11] M. Yousefieh, M. Shamanian, and A. Saatchi, Optimization of Experimental Conditions of the Pulsed Current GTAW Parameters for Mechanical Propeties of SDSS UNS S32760 Welds based on the Taguchi Design Method. J. Mater. Eng. Perform.21(2012)1978-1988

[12] P.J. Ross, Taguchi Techniques for Quality Engineering ,McGraw-Hill, New York, 1988.

[13] M. Yousefieh, M. Shamanian, A. Saatchi, Optimization of the pulsed current gas tungsten arc welding (PCGTAW) parameters for corrosion resistance of super duplex stainless steel (UNS S32760) welds using the Taguchi method. J. Alloys Compd.509(2011) 782-788.

[14] M. Yousefieh, M. Shamanian, A.R. Arghavan, Analysis of Design of Experiments Methodology for Optimization of Pulsed Current GTAW Process Parameters for Ultimate Tensile Strength of UNS S32760 Welds. Metallogr. Microstruct. Anal. 1(2012) 85–91.